Hindawi
Journal of Chemistry
Volume 2022, Article ID 3502872, 8 pages
https://doi.org/10.1155/2022/3502872

Research Article

Acefylline Derivatives as a New Class of Anticancer Agents: Synthesis, Molecular Docking, and Anticancer, Hemolytic, and Thrombolytic Activities of Acefylline-Triazole Hybrids

Irum Shahzadi,[1] Ameer Fawad Zahoor,[1] Bushra Parveen,[1] Azhar Rasul,[2] Zohaib Raza,[3] Sajjad Ahmad,[4] Ali Irfan,[1] and Gamal A. El-Hiti[5]

[1]*Department of Chemistry, Government College University Faisalabad, Faisalabad 38000, Pakistan*
[2]*Department of Zoology, Government College University Faisalabad, Faisalabad 38000, Pakistan*
[3]*Department of Pharmacology, Government College University Faisalabad, Faisalabad 38000, Pakistan*
[4]*Department of Chemistry, University of Engineering and Technology Lahore, Faisalabad Campus, Faisalabad 38000, Lahore, Pakistan*
[5]*Cornea Research Chair, Department of Optometry, College of Applied Medical Sciences, King Saud University, Riyadh 11433, Saudi Arabia*

Correspondence should be addressed to Ameer Fawad Zahoor; fawad.zahoor@gcuf.edu.pk and Gamal A. El-Hiti; gelhiti@ksu.edu.sa

Received 3 March 2022; Revised 11 May 2022; Accepted 12 May 2022; Published 2 June 2022

Academic Editor: Dharmendra Kumar Yadav

The synthesis of novel acefyllines and exploring their biological activities attract researchers due to their medicinal applications. Therefore, the current work reports the successful synthesis of a series of novel acefyllines in good yields, and their structures were confirmed using various spectroscopic methods. The synthesized acefyllines demonstrated moderate activity (cell viability = 22.55 ± 0.95% − 57.63 ± 3.65%) compared with the starting drug acefylline (cell viability = 80 ± 3.87%) against the human liver carcinoma (Hep G2 cell line). *N*-(4-Chlorophenyl)-2-(4-(3,4-dichlorophenyl)-5-((1,3-dimethyl-2,6-dioxo-2,3-dihydro-1*H*-purin-7(6*H*)-yl)methyl)-4*H*-1,2,4-triazol-3-ylthio)acetamide exhibited the most potent activity (cell viability = 22.55 ± 0.95%) among the synthesized derivatives. The *in silico* modeling studies were performed to predict the binding of the most potent derivative with a binding site that agreed with the results of the antiproliferative activity. The newly synthesized heterocycles exhibited the least hemolytic and moderate clot lysis activity.

1. Introduction

The most common type of liver cancer is hepatocellular carcinoma (HCC) which is the third leading cause of death in humans due to cancer [1]. Only 11% of cancerous cells are cured with chemotherapy, 49% with surgery, and 40% with radiotherapy [2]. Different chemotherapeutic drugs are available but are expensive, have negative side effects, and are not very effective. Therefore, in the search for anticancer drugs, there is a considerable surge in the design and development of novel agents [3, 4].

Recently, various pyrimidine and caffeine derivatives have been successfully synthesized, and their biological activities were evaluated [5–7]. Pyrimidine-containing compounds have many pharmacological applications and have been found to be active against pathogens [8–10]. For example, theophylline or methylxanthine (1; Figure 1) belongs to a class of xanthine alkaloids, which grabs great attention because of its extensive therapeutic use to treat respiratory disorders such as chronic obstructive pulmonary disease (COPD) and asthma [11]. Asthma is a heterogeneous syndrome with airway inflammation that remained under consideration by scientists, and many efforts have been made for its treatment. Among various medications, theophylline derivatives have played a remarkable role. For example, 8-anilide theophylline derivatives were synthesized

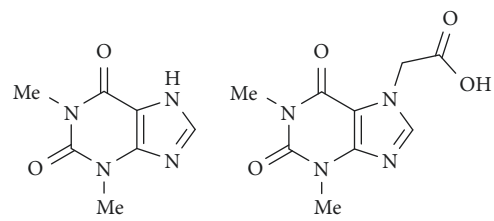

Figure 1: Structures of theophylline (**1**) and acefylline (**2**).

and were found to be effective [12, 13]. It is a bronchodilator drug that relaxes stiffer muscles and open-air passageways [14]. Moreover, it possesses anti-inflammatory properties that suppress the hyperinflation of airways and reduce the chances of dyspnea [15].

The efficiency of theophylline (**1**) as an anti-inflammatory agent varies with the nuclear factor-KB, phosphodiesterase certification, and apoptosis [16]. To treat COPD, it shows anti-inflammatory activity by inhibition of activated inflammatory genes [17]. Theophylline (**1**) not only inhibits the mediators of the inflammatory process but also inhibits the production of oxygen-free radicals. Theophylline (**1**) pharmaceutical activity, as a bronchodilator and anti-inflammatory drug *in vivo*, affects the glucocorticoid receptors that ultimately reduce THF-A concentration [18]. Moreover, 1 sugar hydrazones were found to be effective and have antimicrobial potencies against Aspergillus fumigatus (AF) and Penicillium italicum (PI) [19]. However, 1 is a second-line bronchodilator due to its narrow therapeutic range and index along with side effects such as insomnia, nausea, and vomiting [20].

Acefylline derivatives exhibit important biological activities and belong to the bronchodilators class of drugs. Along with bronchodilation, acefylline derivatives are also reported to exhibit potent activities such as anticancer [21], antituberculosis [22], and antiasthmatic activities [23]. Moreover, they have a cardiac stimulant [24], and adenosine antagonist receptor [25], and therefore, acefylline (**2**; Figure 1) has become attractive for researchers.

Recently, we have reported the activity of 1,3,4-oxadiazoles [26] and 1,2,4-triazoles [27] derived from **2** as potential anticancer drug candidates. Considering the importance and anticancer activity of 1,2,4-triazoles, we have considered the synthesis of a new series of acefyllines that have different aryl groups and evaluated their anticancer activity. In addition, to explore what effect the aryl group in compounds **8** could have on the reactivity of the synthesized derivatives **9**.

2. Materials and Methods

2.1. Materials and Methods. Analytical grade reagents were purchased from Alfa Aesar (Kandel, Germany) and Merck (Gillingham, UK) and used without further purification. The synthesized compounds were purified using the recrystallization technique or column chromatography. IR spectra were obtained on Bruker FTIR spectrometer (Bruker, Zürich, Switzerland) using KBr discs. The NMR spectra were accessed using Bruker Spectrometer model AV-400 (Bruker, Zürich, Switzerland) at 400 MHz for ^{1}H and 100 MHz for ^{13}C spectra. Deuterated dimethyl sulfoxide (DMSO-d_6) was used as a solvent, and chemical shift values were recorded in ppm. The melting points were evaluated using the Gallenkamp apparatus. The glass column filled with grade 60 silica gel was used for column chromatography. The TLC was performed using analytical grade solvents on silica gel-coated TLC plates (60 F254). The progress of reactions was monitored using TLC plates, and the spots were checked under UV light.

*2.2. General Procedure for the Synthesis of Acefylline Derivatives **9a**–**9e**.* Compounds **9a**–**9e** were synthesized according to the reported procedures [26–28]. A mixture of appropriate triazole (0.2 g, 0.45 mmol) and pyridine (0.12 g, 1.5 mmol) in DCM (10 mL) was stirred for 15 minutes. 2-Bromo-*N*-phenyl/arylacetamide (0.46 g, 2.0 mmol) was added, and the reaction mixture was stirred for 24–48 h at 25°C. After reaction completion, *n*-hexane (15 mL) was added to the reaction mixture, and the resulting solids were collected by filtration. The solids were purified by recrystallization using EtOH.

*2.2.1. 2-(4-(3,4-dichlorophenyl)-5-((1,3-dimethyl-2,6 dioxo-1,2,3,6-tetrahydro-7H-purin-7-yl methyl)-4H-1,2,4-triazol-3-yl)thio)-N-phenylacetamide (**9a**).* Cream powder; yield: 71%; m.p 209°C; IR (KBr): ν 3349 (N-H), 1648 (C=O), 1639 (C=O), 1541 (C=N), 1454 (C=C). ^{1}H NMR (δ/ppm): 3.14 (s, 3H, Me), 3.39 (s, 3H, Me), 4.15 (s, 2H, SCH_2), 5.66 (s, 2H, NCH_2), 7.19–7.80 (m, 8H, Ar), 7.98 (s, 1H, CH), 9.96 (s, 1H, NH). ^{13}C NMR (δ/ppm): 27.9 (Me), 29.9 (Me), 37.3 (SCH_2), 41.2, (NCH_2), 106.5, 115.1, 119.6, 121.1, 124.0, 127.5, 129.2, 132.4, 133.1, 138.3, 139.2, 143.3, 143.5, 148.4, 151.6, 151.8, 154.6 (C=O), 165.8 (C=O). MS *m*/*z* (ES^+) 570.0748 (M^+) (100%). Anal. Calcd. For $C_{24}H_{20}Cl_2N_8O_3S$: C, 50.45; H, 3.53; N, 19.61; found: C, 50.24; H, 3.64; N, 19.40%.

*2.2.2. 2-(4-(3,4-dichlorophenyl)-5-((1,3 dimethyl-2,6-dioxo-1,2,3,6-tetrahydro-7H-purin-7-yl)methyl)-4H-1,2,4-triazol-3-yl)thio)-N-(2-fluorophenyl)acetamide (**9b**).* Light brown, amorphous solid; yield: 69%; m.p 180°C; IR (KBr): ν 3349 (N-H), 1648 (CO), 1639 (C=O), 1541 (C=N), 1454 (C=C). ^{1}H NMR (δ/ppm): 3.46 (s, 3H, Me), 3.46 (s, 3H, Me), 4.15 (s, 2H, SCH_2), 5.65 (s, 2H, NCH_2), 7.15–7.86 (m, 8H, Ar), 7.98 (s, 1H, CH), 10.01 (s, 1H, NH). ^{13}C NMR (δ/ppm): 27.9 (Me), 29.9 (Me), 37.2 (SCH_2), 41.4, (NCH_2), 110.8, 119.6, 120.8, 127.5, 130.5, 131.2, 132.4, 132.6, 139.3, 141.2, 143.5, 146.7, 148.4, 149.4, 151.7, 151.3, 151.4, 151.9, 154.6 (C=O), 165.8 (C=O). MS *m*/*z* (ES^+) 588.0642 (M^+) (100%). Anal. Calcd. For $C_{24}H_{19}Cl_2FN_8O_3S$: C, 48.91; H, 3.25; N, 19.01%; found: C, 48.84; H, 3.16; N, 19.20%.

*2.2.3. 2-(4-(3,4-dichlorophenyl)-5-((1,3 dimethyl-2,6-dioxo-1,2,3,6-tetrahydro-7H-purin-7-yl)methyl)-4H-1,2,4-triazol-3-yl)thio)-N-(2-methoxyphenyl)acetamide (**9c**).* Light brown, amorphous solid; yield: 64%; mp 175°C; IR (KBr): ν 3349

(N-H), 1648 (C=O), 1639 (C=O), 1541 (C=N), 1454 (C=C). ^{1}H NMR (δ/ppm): 3.13 (s, 3H, Me), 3.40 (s, 3H, Me), 3.81 (s, 3H, OMe), 4.12 (s, 2H, SCH_2), 5.65 (s, 2H, NCH_2), 6.89–7.76 (m, 7H, Ar), 8.00 (s, 1H, CH), 9.60 (s, 1H, NH). ^{13}C NMR (δ/ppm): 27.9 (Me), 29.9 (Me), 37.4 (SCH_2), 41.4, (NCH_2), 62.2 (OMe), 106.5, 119.6, 121.1, 124.0, 127.5, 129.2, 130.5, 130.7, 132.4, 132.7, 139.2, 143.5, 148.4, 148.7, 150.1, 151.4, 151.6, 151.8, 154.6 (C=O), 165.8 (C=O). MS m/z (ES^+) 600.0667 (M^+) (100%). Anal. Calcd. For $C_{25}H_{22}Cl_2N_8O_4S$: C, 49.92; H, 3.69; N, 18.63%; found: C, 49.84; H, 3.86; N, 19.50%.

*2.2.4. N-(2-chlorophenyl)-2-(4-(3,4 dichlorophenyl)-5-((1,3-dimethyl-2,6 dioxo-1,2,3,6-tetrahydro-7H-purin-7-Yl)methyl)-4H-1,2,4-triazol-3-yl)thio)acetamide (**9d**).* Off white, amorphous solid; yield: 65%; m.p 240°C; IR (KBr): ν 3349 (N-H), 1648 (C=O), 1639 (C=O), 1541 (C=N), 1454 (C=C). ^{1}H NMR (δ/ppm): 3.14 (s, 3H, Me), 3.39 (s, 3H, Me), 4.15 (s, 2H, SCH_2), 5.66 (s, 2H, NCH_2), 7.19–7.80 (m, 7H, Ar), 7.98 (s, 1H, CH), 9.86 (s, 1H, NH). ^{13}C NMR (δ/ppm): 27.9 (Me), 29.9 (Me), 37.2 (SCH_2), 41.4, (NCH_2), 106.5, 110.8, 119.6, 120.8, 127.4, 130.5, 131.2, 132.4, 132.5, 139.3, 143.5, 146.7, 147.3, 148.4, 149.4, 151.3, 151.4, 151.9, 154.6 (C=O), 165.8 (C=O). MS m/z (ES^+) 604.0366 (M^+) (100%). Anal. Calcd. For $C_{24}H_{19}Cl_3N_8O_3S$: C, 47.58; H, 3.16; N, 18.49%; found: C, 48.24; H, 3.06; N, 19.30%.

*2.2.5. N-(4-chlorophenyl)-2-(4-(3,4 dichlorophenyl)-5-((1,3-dimethyl-2,6 dioxo-1,2,3,6-tetrahydro-7H-purin-7-Yl) methyl)-4H-1,2,4-triazol-3-yl)thio)acetamide (**9e**).* Off white, amorphous solid; yield: 73%; m.p 176°C; IR (KBr) ν 3349 (N-H), 1648 (C=O), 1639 (C=O), 1541 (C=N), 1454 (C=C). ^{1}H NMR (δ/ppm): 3.14 (s, 3H, Me), 3.40 (s, 3H, Me), 4.15 (s, 2H, SCH_2), 5.65 (s, 2H, NCH_2), 7.15–7.86 (m, 7H, Ar), 7.98 (s, 1H, CH), 10.09 (s, 1H, NH). ^{13}C NMR (δ/ppm): 27.9 (Me), 29.9 (Me), 37.4 (SCH_2), 41.4, (NCH_2), 106.5, 119.6, 121.1, 124.0, 127.4, 129.2, 129.4, 130.4, 130.8, 132.4, 139.2, 143.5, 148.4, 148.7, 150.1, 151.4, 151.6, 151.8, 154.6 (C=O), 165.8 (C=O). MS m/z (ES^+) 604.0366 (M^+) (100%). Anal. Calcd. For $C_{24}H_{19}Cl_3N_8O_3S$: C, 47.58; H, 3.16; N, 18.49%; found: C, 47.44; H, 3.16; N, 19.30%.

2.3. Biological Evaluation

2.3.1. MTT Assay. The cytotoxic potential of the synthesized compounds was tested according to the MTT assay [29]. The synthesized compounds were tested against the cancer cell line Hep G2. The cell line was developed as a monolayer culture in the Dulbecco's modified Eagle's medium having FBS (10%) and streptomycin (1%)/penicillin (100 μg/mL). It was incubated in a humid atmosphere having carbon dioxide (5%) and air (95%) and water at 37°C. The cell line (Hep G2) was treated with a suitable concentration (100 μg/100 mL), a solution of synthesized compounds in DMSO. Cells treated with DMSO were used as a negative control in all experiments. The Hep G2 cells were cultured overnight in 96-well plates and further treated with the synthesized compounds (at different concentrations) and incubated for 48 h. After that added MTT reagent (10 μl, 5 mg/mL) to each plate, followed by incubation for 4 h at 37°C. Finally, DMSO (150 μl) was added to each plate to calculate the percentage cell viability by measuring the absorbance at 490 nm *via* a microplate reader.

2.3.2. Hemolytic Assay. A sample of human blood (3 mL) was taken and centrifuged ($1000 \times g$) for 5 minutes. Erythrocytes were isolated which was dissolved in a phosphate buffer (pH 7.4). A solution of the synthesized compound (20 μL; 10 mg/mL) was added to the RBC suspension (180 μL) followed by incubation for 30 min at 37°C. The ABTS and DMSO were taken as positive and negative controls, respectively. The age hemolysis (%) was calculated using the following equation [30]:

$$\text{agehemolysis}(\%) = \frac{\text{Absorbance of sample} - \text{Absorbance of DMSO}}{\text{Absorbance of ABTS}} \times 100. \quad (1)$$

2.3.3. Thrombolytic Assay. A sample of human blood (1 mL) was incubated for 45 minutes at 25°C in a preweighed tube. After the formation of the clot, the serum was completely removed, and each tube was weighed again to find out the weight of the clot. A solution (100 μL) of each of the tested compounds was added separately and kept at 37°C for 3 hours, and clot lysis in the sample was observed. DMSO was added in some tubes (as a negative thrombolytic control) while ABTS was used as a positive control. After the clot lysis, the tubes were weighed, and the difference in weights was calculated. The percentage of thrombolysis was calculated using the following equation[31]:

$$\text{Clotlysis}(\%) = \frac{\text{Initial clot weight} - \text{Final clot weight}}{\text{Initial weight of the clot}} \times 100. \quad (2)$$

2.3.4. Molecular Docking. Compound **9e** was further *in silico* modeled to complement its experimental studies to further delineate its potential mechanism of action responsible for its anticancer activity. Compound **9e** was screened through the PASS prediction tool that predicts the therapeutic target of the tested molecule (≥95% accuracy) and anticancer target with the probability of activity (Pa) > 50%. It was molecularly docked against the target by using the induced fit docking protocol at the platform of molecular operating environment 2015.10. The chemical structures of compounds were sketched, and energy was minimized under the CHARMM force field utilizing MMFF9x partial charge in Discovery Studio Visualizer 17.2. The three-dimensional (3D) X-ray structure of crystalized STAT3 (PDB ID:5AX3, 2.984 Å) was obtained from RSCB Protein Data Bank (http://www.rscb.org) and corrected and optimized via

QuickPrep function of MOE for structural issues, such as missing residues, protonation state, alternates, and termini capping. The Amber10: EHT force field was utilized to minimize the energy of the molecular environment. The Site Finder module of MOE was utilized to identify, isolate, and optimize the small molecules binding pocket within the STAT3 hotspot. The docking of the compounds was performed in the binding pocket by Dock module utilizing Triangle Matcher placement methods, scored with London ΔG scoring function. The poses were further redocked with the induced fit refinement method, and binding modes were rescored with GBVI/WSA ΔG scoring function. The poses utilizing the lowest binding energy (ΔG) were simulated for ligand-protein interactions via Discovery Studio Visualizer 17.2.

3. Results and Discussion

3.1. Chemistry. The synthesis of thio*N*-phenylacetamide 3,4-dichlorophenyl-1,2,4-triazoles of acefylline **9a–9e** is presented in Scheme 1. Firstly, the esterification of **2** was performed to afford compound **3** in 76% yield followed by reaction with hydrazine hydrate to give **4** in 96% yield. Treatment of **4** with 3,4-dichlorophenyl isothiocyanate (**5**) gave the intermediate **6** which on treatment aqueous potassium hydroxide (KOH) under reflux condition afforded **7** in 71% yield. Alkylation of **7** with various substituted bromoacetamides **8a–8e** in dichloromethane (DCM) containing pyridine at room temperature gave the final products **9a–9e** in 64–73% yield.

*3.2. Elucidation of Acefylline **9a–9e** Structures.* The structures of the newly synthesized heterocycles were confirmed using various spectroscopic techniques (see the experimental section for details). The FTIR spectra of compound **9a–9e** showed the presence of two different carbonyl groups. The ^{1}H NMR spectra showed the presence of an exchange singlet that appeared within the 9.60–10.09 ppm region due to the amide proton. The CH=N proton appeared as a singlet at 7.98 ppm. The protons of the two methyl groups appeared as two singlets at 3.14 and 3.39–3.46 ppm regions. The ^{13}C NMR spectra of compound **9a–9e** showed the presence of two different carbonyl groups that appeared down fielded at 154.6 and 165.8 ppm. In addition, they show the presence of two different methyl groups (27.9 and 29.9 ppm). The NMR spectra of compound **9c** showed the presence of the methoxy group that appeared at 3.81 for the protons and at 62.2 ppm for the carbon. Additionally, the structures of **9a–9e** were confirmed by the data obtained from the high-resolution mass spectra and elemental analyses. The NMR spectra of **9a–9e** are shown in Figures S1–S10.

3.3. Anticancer Activity. The inhibitory potential of compounds **9a–9e** against the proliferation of Hep G2 cancer cell line was accessed using the MTT assay and was compared with that obtained for **2**. The results showed that compounds **9a–9e** were more reactive against cancer cells (cell viability = 22.55 ± 0.95% to 57.63 ± 3.65%) compared with **2** (cell viability = 80 ± 3.87%). Compound **9e** showed the most potent antiproliferative activity (cell viability = 22.55 ± 0.95%). Compounds **9a–9d** showed moderate activity against the liver cancer cell line Hep G2 (cell viability 53.85 ± 3.30%, 47.66 ± 3.59%, 53.49 ± 1.97%, and 57.63 ± 3.65%, respectively). The anticancer activity of **9e** was also tested at different concentrations that ranged from 0.3 μg to 200 μg, and the best activity was observed at the highest concentration (200 μg; Figure 2). For compound **9e**, the $IC_{50}$was calculated as 5.23 ± 0.95 μM.

3.4. The Structure-Activity Relationship (SAR). The biological activities of compounds **9a–9e** along with that for **2** and controls are summarized in Table 1. Compound **9a** which contains a phenyl group as a substituent showed a moderate activity (cell viability = 53.85 ± 3.30%) against the liver cancer cell lines Hep G2. Compound **9e** which contains an electron-withdrawing group (4-Cl) showed the greatest potential (cell viability = 22.55 ± 0.95%) against the cancer cells compared to the other derivatives. The activity of compounds **9b**, **9c**, and **9d** which contain electron-withdrawing substituents (2-F, 2-OMe, and 2-Cl, respectively) were relatively low. Clearly, the presence of the electron-withdrawing group (e.g., Cl) at the 4-position of the phenyl ring might be responsible for a greater binding activity with the cancer cell.

3.5. Hemolytic Activity. The results of the hemolytic activity indicated that compounds **9a–9e** were less toxic compared with **2**. Moderate activity was observed for compound **9a** (4.7%) which contains unsubstituted phenyl ring compared with **2** (43.5%). Compounds **9b–9e** had electron-withdrawing substituents on the phenyl ring and appeared to be the least toxic with hemolysis (%) of 1.86, 2.87, 0.23, and 1.20, respectively.

3.6. Thrombolytic Activity. Compounds **9a–9e** exhibited low-to-moderate clot lysis activity. Compounds bearing electron-withdrawing substituents at the phenyl ring exhibited a moderate clot lysis activity [**9a** (39%), **9d** (37%), and **9e** (26%)] which is much higher than that for acefylline (2; 6.85%). The maximum activity was observed for compounds **9b** and **9c** that have electron-withdrawing substituents at the *ortho*-position of the phenyl ring (thrombolysis (%) = 48.0 and 49.4, respectively).

3.7. Molecular Docking Analysis. The *in silico* studies were carried out for the prediction and elucidation of the potential mechanism for the inhibitory action of compound **9e** for its superior anticancer activity in the experimental studies. The PASS predictions resulted in STAT3 as a potential therapeutic anticancer target of compounds **9e** with *Pa*~ 0.51. Compound **9e** structure-activity relationship was investigated *via* the induced fit docking protocol using STAT3 hotspot. It has a superior binding affinity (−7.9 ΔG kcal/mol) as compared to **2** binding affinity (−5.32 ΔG kcal/mol). The binding energy and the interaction profile of compounds **2** and **9e** are shown in Table 2.

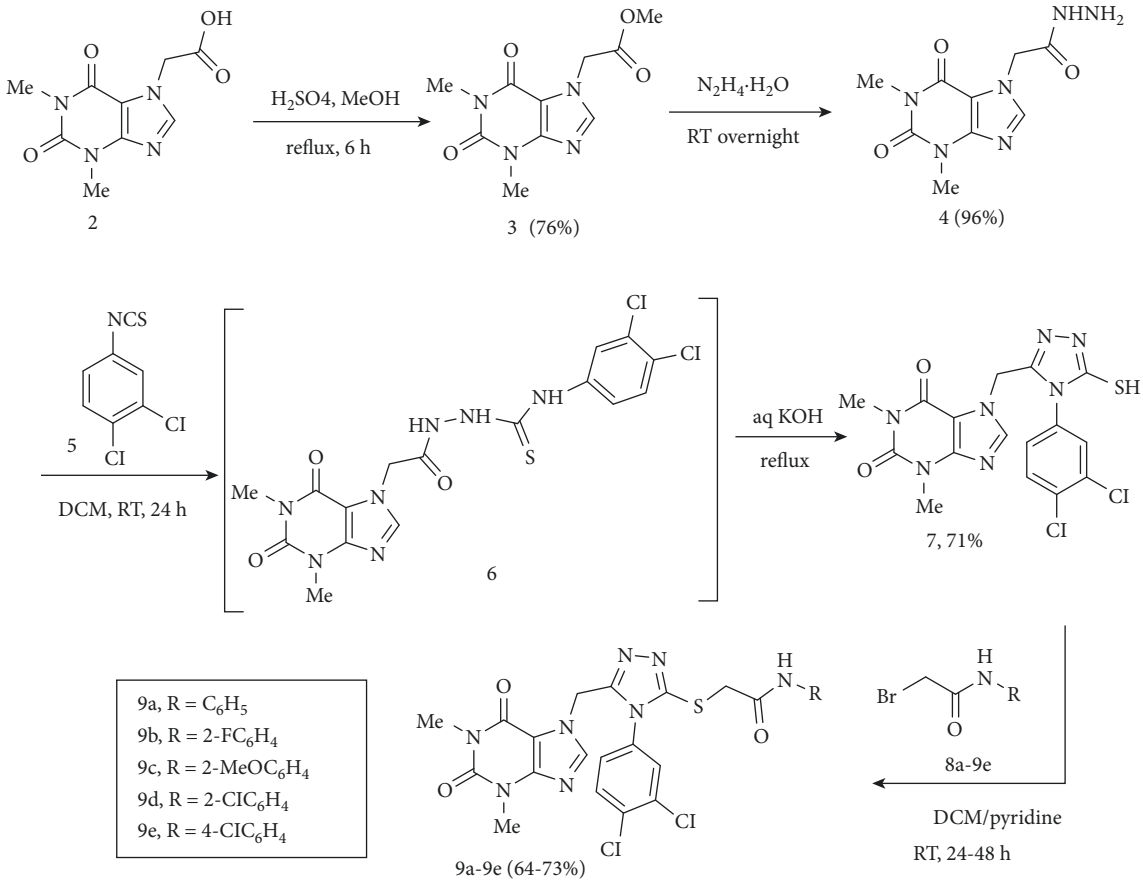

Scheme 1: Synthesis of acefylline **9a–9e**.

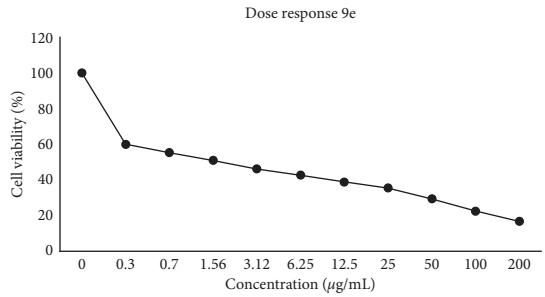

Figure 2: Effect of concentration of **9e** on the cell viability (%).

The binding pocket of the STAT3 hotspot comprised the LYS352, TYR353, LEU355, THR150, THR151, ALA356, LYS351, TYR306, GLU72, ASP308, TYR122, ARG126, GLN123, and ASP311 (Figure 3). The binding mode analysis revealed that both **2** and **9e** efficiently stabilized their confirmation within the three-dimensional space of STAT3. The conformational analysis of **2** suggested its stable confirmation at the binding pocket and interacted with vital residues which may destabilize the hotspot. Compound **9e** was found to orient its confirmation more towards the STAT3 residues, which may suggest its preferential inhibition of STAT3 complexation.

Acefylline (2) stabilized its confirmation mainly with the H-bonding through the binding with TYR306, ASP311, GLU72, LYS352, GLN123, and ASN73 (Figure 4). In addition, it stabilizes itself through the hydrophobic interaction with the TYR306 and pi-cation and pi-anion interactions with the ASP311 and LYS352 although compound **9e** shared the interactions with the majority of residues conserved for **2** interactions, with different bonding interactions that may suggest its superior binding affinity and stabilization at STAT3 hotspot. Compound **9e** established H-bond with the TYR122, ASP308, LYS352, GLU72, TYR306, pi-cation, and pi-anion interactions with the ASP311, ARG126, LYS351, and hydrophobic interactions with the LYS351 which led its orientation more towards STAT3 hotspot to inhibit its complexation.

The *in silico* studies were performed further to elucidate the anticancer activity of **9e** and to explore the potential structure-activity relationship complementing the

Table 1: Biological activities of **9a**–**9e** along with that for **2**, solvent, and ABTS.

Compounds	*R*	Cell viability*	Hemolysis (%)	Thrombolysis (%)
9a	pH	53.85 ± 3.30	4.70	39.0
9b	2-FC_6H_4	47.66 ± 3.59	1.86	48.0
9c	2-$MeOC_6H_4$	53.49 ± 1.97	2.87	49.4
9d	2-ClC_6H_4	57.63 ± 3.65	0.23	37.0
9e	4-ClC_6H_4	22.55 ± 0.95	1.20	26.0
Acefylline **(2)**		79.00 ± 2.54	43.5	6.85
DMSO		100 ± 0	0.01	0.57
ABTS		—	95.50	88.0

Note. *Cell viability (Mean ± SD), (triplicate, 100 μg/mL).

Table 2: The docking parameters of **2** and **9e** using the STAT3 hotspot.

Compound	Binding energy ΔG (kcal/mol)	Interacting residues	Interaction type
2	−5.32	ASP311, GLU72, TYR306, LYS352, GLN123, and ASN73	H-bond, π-anion, π-cation, π-alkyl, and π-σ
9e	−7.9	ASP308, TYR122, ASP311, ARG126, LYS352, GLU72, TRY306, and LYS351	H-bond, π-anion, π-cation, and π-alkyl

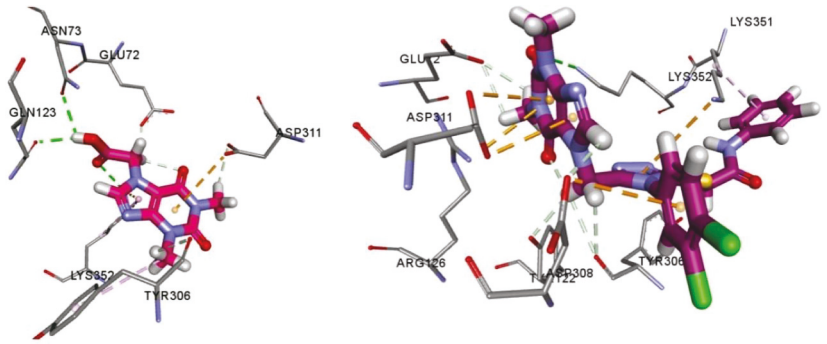

(a) (b)

Figure 3: Conformational analysis of compounds docked using STAT3 hotspot; simulated best binding mode of (a) **2** and (b) **9e** at binding pocket.

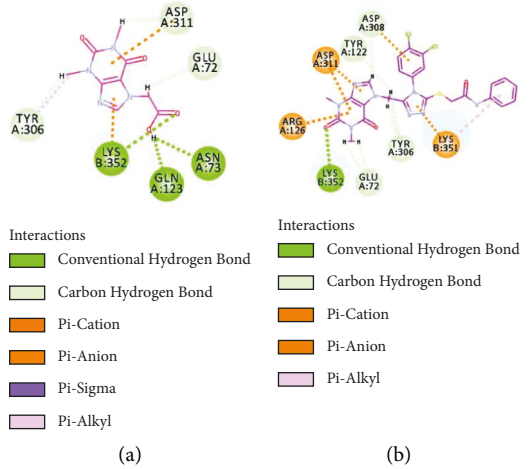

(a) (b)

Figure 4: Interaction within the binding pocket of STAT3 hotspot of (a) **2** and (b) **9e**. Two-dimensional (2D) perspective on docked compounds' interaction with STAT3 key residues illustrated as balls and sticks colored by type of interaction.

experimental studies. The STAT3 was identified as the potential target of **9e** for anticancer activity by the PASS prediction. The binding affinity of **9e** to STAT3 was evaluated using the induced fit docking protocol to simulate its complexation, binding mode, and the interactions that reliably simulate the flexibility of the binding pocket upon ligand binding. Compound **9e** was found to bind and disrupt the STAT3 hotspot with superior binding affinity as compared to **2**. Interestingly, **9e** exhibited an improved binding affinity well aligned with the experimental studies as compared to its previous analog [26]. Moreover, the stable orientation of **9e** allowed it to establish diverse interactions with key residues of the STAT3 hotspot and orient it more towards the STAT3 to inhibit its complexation. Clearly, **9e** has a more potent anticancer activity compared with **2**.

4. Conclusions

Nine novel acefyllines containing 3,4-dichlorophenyl-1,2,4-triazole hybrids were synthesized in high yields, and their structures were confirmed. The synthesized acefyllines were tested *in vitro* for their anticancer activity for the human liver cancer cell line (Hep G2) using the MTT assay. The synthesized acefyllines exhibited moderate activity against the Hep G2. *N*-(4-chlorophenyl)-2-(4-(3,4-dichlorophenyl)-5-((1,3-dimethyl-2,6-dioxo-2,3-dihydro-1*H*-purin-7(6*H*)-yl) methyl)-4*H*-1,2,4-triazol-3-ylthio)acetamide (**9e**) was found to be the most active derivative among the synthesized ones with a cell viability of 22.55 ± 0.95%. The cytotoxic potential of acefyllines was confirmed by evaluating their hemolysis and thrombolysis potentials and was found to exhibit low toxicity and excellent thrombolytic activity.

Data Availability

Data are contained in the article and the supplementary material.

Conflicts of Interest

The authors have no conflicts of interest.

Acknowledgments

El-Hiti is grateful to the Deanship of Scientific Research, King Saud University, for funding through the Vice Deanship of Scientific Research Chairs. The authors acknowledge Government College University Faisalabad for support and facilities to carry out the work.

Supplementary Materials

Figure S1: ^{1}H NMR spectrum of **9a**, Figure S2: ^{13}C NMR spectrum of **9a**, Figure S3: ^{1}H NMR spectrum of **9b**, Figure S4: ^{13}C NMR spectrum of **9b**, Figure S5: ^{1}H NMR spectrum of **9c**, Figure S6: ^{13}C NMR spectrum of **9c**, Figure S7: ^{1}H NMR spectrum of **9d**, Figure S8: ^{13}C NMR spectrum of **9d**, Figure S9: ^{1}H NMR spectrum of **9e**, and Figure S10: ^{13}C NMR spectrum of **9e**. (*Supplementary Materials*)

References

[1] E. Kim and P. Viatour, "Hepatocellular carcinoma: old friends and new tricks," *Experimental and Molecular Medicine*, vol. 52, no. 12, pp. 1898–1907, 2020.

[2] R. A. Sharma, R. Plummer, J. K. Stock et al., "Clinical development of new drug-radiotherapy combinations," *Nature Reviews Clinical Oncology*, vol. 13, no. 10, pp. 627–642, 2016.

[3] M. Arruebo, N. Vilaboa, B. Sáez-Gutierrez et al., "Assessment of the evolution of cancer treatment therapies," *Cancers*, vol. 3, no. 3, pp. 3279–3330, 2011.

[4] V. Prachayasittikul, R. Pingaew, N. Anuwongcharoen et al., "Discovery of novel 1,2,3-triazole derivatives as anticancer agents using QSAR and in silico structural modification," *SpringerPlus*, vol. 4, no. 1, p. 571, 2015.

[5] A. A. Abu-Hashem and H. A. R. Hussein, "Synthesis and antitumor activity of new pyrimidine and caffeine derivatives," *Letters in Drug Design and Discovery*, vol. 12, no. 6, pp. 471–478, 2015.

[6] A. A. Abu-Hashem and S. A. Al-Hussain, "Design, synthesis of new 1,2,4-triazole/1,3,4-thiadiazole with spiroindoline, imidazo[4,5-*b*]quinoxaline and thieno[2,3-*d*]pyrimidine from isatin derivatives as anticancer agents," *Molecules*, vol. 27, no. 3, p. 835, 2022.

[7] A. A. Abu-Hashem, S. A. Al-Hussain, and M. E. A. Zaki, "Design, synthesis and anticancer activity of new polycyclic: Imidazole, thiazine, oxathiine, pyrrolo-quinoxaline and thienotriazolopyrimidine derivatives," *Molecules*, vol. 26, no. 7, p. 2031, 2021.

[8] A. A. Abu-Hashem, "Synthesis and biological activity of pyrimidines, quinolines, thiazines and pyrazoles bearing a common thieno moiety," *Acta Poloniae Pharmaceutica - Drug Research*, vol. 75, no. 1, pp. 59–70, 2018.

[9] A. A. Abu-Hashem, K. M. Abu-Zied, and M. F. El-Shehry, "Synthetic utility of bifunctional thiophene derivatives and antimicrobial evaluation of the newly synthesized agents," *Monatshefte für Chemie - Chemical Monthly*, vol. 142, no. 5, pp. 539–545, 2011.

[10] R. Merugu, S. Garimella, D. Balla, and K. Sambaru, "Cheminform abstract: synthesis and biological activities of pyrimidines: a review," *ChemInform*, vol. 47, no. 29, pp. 88–93, 2016.

[11] R. L. ZuWallack, D. A. Mahler, D. Reilly et al., "Salmeterol plus theophylline combination therapy in the treatment of COPD," *Chest*, vol. 119, no. 6, pp. 1661–1670, 2001.

[12] A. K. M. Hayallah, A. A. Talhouni, and A. A. M. A. Alim, "Design and synthesis of new 8-anilide theophylline derivatives as bronchodilators and antibacterial agents," *Archives of Pharmacal Research*, vol. 35, no. 8, pp. 1355–1368, 2012.

[13] L. Profire, V. Sunel, D. Lupascu, M. C. Baican, N. Bibire, and C. Vasile, "New theophylline derivatives with potential pharmacological activity," *Farmacia*, vol. 58, no. 2, pp. 170–176, 2010.

[14] S. Lim, A. Jatakanon, D. Gordon, C. Macdonald, K. F. Chung, and P. J. Barnes, "Comparison of high dose inhaled steroids, low dose inhaled steroids plus low dose theophylline, and low dose inhaled steroids alone in chronic asthma in general practice," *Thorax*, vol. 55, no. 10, pp. 837–841, 2000.

[15] S. R. Tapadar, M. Das, A. D. Chaudhuri, S. Basak, and A. B. S. Mahapatra, "The effect of acebrophylline vs sustained release theophylline in patients of copd- a comparative study," *Journal of Clinical and Diagnostic Research*, vol. 8, no. 9, 2014.

[16] B. G. Cosio, A. Iglesias, A. Rios et al., "Low-dose theophylline enhances the anti-inflammatory effects of steroids during

exacerbations of COPD," *Thorax*, vol. 64, no. 5, pp. 424–429, 2009.

[17] P. J. Barnes, "American journal of respiratory and critical care medicine," *Theophylline*, vol. 188, no. 8, pp. 901–906, 2013.

[18] S. Watanabe, J. Yamakami, M. Tsuchiya, T. Terajima, J. Kizu, and S. Hori, "Anti-inflammatory effect of theophylline in rats and its involvement of the glucocorticoid-glucocorticoid receptor system," *Journal of Pharmacological Sciences*, vol. 106, no. 4, pp. 566–570, 2008.

[19] M. A. Mosselhi, M. A. Abdallah, N. H. Metwally, I. A. El-Desoky, and L. M. Break, "Synthesis, structure and antimicrobial evaluation of new derivatives of theophylline sugar hydrazones," *Arkivoc*, vol. 2009, no. 14, pp. 53–63, 2010.

[20] D. Shukla, S. Chakraborty, S. Singh, and B. Mishra, "Doxofylline: a promising methylxanthine derivative for the treatment of asthma and chronic obstructive pulmonary disease," *Expert Opinion on Pharmacotherapy*, vol. 10, no. 14, pp. 2343–2356, 2009.

[21] A. B. Zlatkov, P. T. Peikov, G. C. Momekov, I. Pencheva, and B. Tsvetkova, "Synthesis, stability and computational study of some ester derivatives of theophylline-7-acetic acid with antiproliferative activity," *Der Pharma Chemica*, vol. 2, no. 6, pp. 197–210, 2010.

[22] Y. Voynikov, V. Valcheva, G. Momekov, P. Peikov, and G. Stavrakov, "Theophylline-7-acetic acid derivatives with amino acids as anti-tuberculosis agents," *Bioorganic and Medicinal Chemistry Letters*, vol. 24, no. 14, pp. 3043–3045, 2014.

[23] K. Aleksandrova, I. Belenichev, A. Shkoda, S. Levich, D. Yurchenko, and N. Buchtiyarova, "Research of antioxidant properties of theophyllinyl-7-acetic acid derivatives," *Oxidants and Antioxidants in Medical Science*, vol. 3, no. 3, pp. 187–194, 2014.

[24] A. Foppoli, L. Zema, A. Gazzaniga et al., "Solid-state chemistry of ambroxol theophylline-7-acetate," *Journal of Pharmaceutical Sciences*, vol. 96, no. 5, pp. 1139–1146, 2007.

[25] B. Tsvetkova, J. Tencheva, and P. Peikov, "Esterification of 7-theophyllineacetic acid with diethylene glycol monomethyl ether," *Acta Pharmaceutica (Zagreb, Croatia)*, vol. 56, no. 2, pp. 251–7, 2006.

[26] I. Shahzadi, A. F. Zahoor, A. Rasul et al., "Synthesis, anticancer, and computational studies of 1, 3, 4-oxadiazole-purine derivatives," *Journal of Heterocyclic Chemistry*, vol. 57, no. 7, pp. 2782–2794, 2020.

[27] I. Shahzadi, A. F. Zahoor, A. Rasul, A. Mansha, S. Ahmad, and Z. Raza, "Synthesis, hemolytic studies, and in silico modeling of novel acefylline-1,2,4-triazole hybrids as potential anticancer agents against mcf-7 and a549," *ACS Omega*, vol. 6, no. 18, pp. 11943–11953, 2021.

[28] S. Faiz, A. F. Zahoor, M. Ajmal et al., "Design, synthesis, antimicrobial evaluation, and laccase catalysis effect of novel benzofuran-oxadiazole and benzofuran-triazole hybrids," *Journal of Heterocyclic Chemistry*, vol. 56, no. 10, pp. 2839–2852, 2019.

[29] R. Akhtar, A. F. Zahoor, A. Rasul, S. Gul Khan, and K. G. Ali, "In-vitro cytotoxic evaluation of newly designed ciprofloxacin-oxadiazole hybrids against human liver tumor cell line (Huh7)," *Pakistan Journal of Pharmaceutical Sciences*, vol. 34, pp. 1143–1148, 2021.

[30] F. Hafeez, A. Mansha, A. F. Zahoor, K. G. Ali, S. G. Khan, and S. A. R. Naqvi, "Facile green approach towards the synthesis of some phenyl piperazine based dithiocarbamates as potent hemolytic and thrombolytic agents," *Pakistan Journal of Pharmaceutical Sciences*, vol. 34, no. 5 (Supplementary), pp. 1885–1890, 2021.

[31] M. Batool, A. Tajammal, F. Farhat et al., "Molecular docking, computational, and antithrombotic studies of novel 1,3,4-oxadiazole derivatives," *International Journal of Molecular Sciences*, vol. 19, no. 11, p. 3606, 2018.